Available online at www.sciencedirect.com
SCIENCE DIRECT®
International Journal of Heat and Mass Transfer 47 (2004) 4995–5009
International Journal of HEAT and MASS TRANSFER
www.elsevier.com/locate/ijhmt

Flow-based control of temperature in long ducts

Sorour Alotaibi [1], Mihir Sen *, Bill Goodwine, K.T. Yang

Department of Aerospace and Mechanical Engineering, University of Notre Dame, Notre Dame, IN 46556, USA

Received 30 December 2003; received in revised form 25 June 2004
Available online 23 August 2004

Abstract

Flow-based control of a thermal system with a long duct and heat loss to the environment is analyzed. A Proportional-Integral controller is used to regulate the duct outlet temperature by using the flow velocity as control input. The one-dimensional energy equation in Eulerian and Lagrangian forms are numerically solved. The non-linear dynamics can be represented by an integral equation in terms of the residence time which acts as a delay. A linear stability analysis leads to a characteristic transcendental equation which is examined for different orders of the residence time. Pontryagin's theorem on the zeros of exponential polynomials is used to obtain stability maps as a function of system parameters. Numerical simulations are performed to verify the predictions, determine super- and sub-critical instabilities, and evaluate the amplitude and frequency of limit-cycle oscillations.

1. Introduction

Control of fluid temperature at a specific location is of importance in many domestic and industrial applications. This is often achieved by transporting fluids such as steam or chilled water through a long duct to distant heat exchangers. In many of these cases, it is desired to have control of the fluid temperature at the outlet by varying its flow rate. The fluid takes time to travel the length of a long duct and, as a result, there is a delay between the inlet and the outlet conditions which affects the dynamics of the system. The effect of this should be taken into account in designing a thermal control system.

Though the effect of delay has been studied in different fields, the literature contains few applications to thermal systems. One early work was that of Munk [1], and since then a small number of papers have appeared in the literature. Heat exchangers have been studied by Górecki and Jekielek [2] and Huang et al. [3]. Zhang and Nelson [4] modeled the effect of a variable-air-volume ventilating system on a building using delay, and Antonopoulos and Tzivanidis [5] developed a correlation for the thermal delay of buildings. In duct flows, Saman and Mahdi [6] analyzed pipe and fluid temperature variations due to flow, and Chow et al. [7] modeled the thermal behavior of fluid conduit flow with transportation delay. The delayed hot water problem has been studied by Comstock [8]. Chu [9] described the application of a discrete optimal tracking controller in an industrial electrical heater with pure delay, and Chu et al. [10] studied a time-delay control algorithm for the same heater. There are also publications on the effect of delay in process engineering such as the book by Ogunnaike and

* Corresponding author. Tel.: +1 574 631 5975; fax: +1 574 631 8341.
E-mail address: mihir.sen.1@nd.edu (M. Sen).
[1] Currently at the Department of Mechanical Engineering, Kuwait University, Safat 13060, Kuwait.

0017-9310/$ - see front matter © 2004 Elsevier Ltd. All rights reserved.
doi:10.1016/j.ijheatmasstransfer.2004.06.017

Nomenclature

A	amplitude of oscillations
c	specific heat at constant pressure [J/kg K]
D	diameter [m]
f	frequency of oscillations
f, g	arbitrary functions
F, F^*	transcendental functions
h	convective heat transfer coefficient [W/m^2 K]
K_p, K_i	constants of PI control
L	length [m]
N	number of divisions for computation
T	temperature
t	time
Δt	time step
v	velocity
x	longitudinal coordinate
Δx	spatial step

Greek symbols

ε	$v\Delta t/\Delta x$
ρ	fluid density [kg/m^3]
σ	eigenvalue
τ	residence time
ω	radian frequency

Subscripts and superscripts

in, out	inlet and outlet, respectively
∞	ambient
$\overline{()}$	steady-state value
r, i	real and imaginary parts, respectively
*	dimensional quantity
$'$	small perturbation

Ray [11] which provides an overview of process dynamics and control.

One-dimensional duct flow can be described by a first-order hyperbolic partial differential equation. This can be solved analytically by the method of characteristics [12,13] or numerically by finite differences [14], Galerkin with Legendre polynomials [15], or orthogonal collocation [16]. Several algorithms have been proposed for control of the different variables. Early research was based on the lumped-parameter model which results in an ordinary differential equation [17] to which control strategies can be applied. Wysocki [16] used orthogonal collocation to control first-order hyperbolic systems. In addition, there have been other applications of control methods for distributed parameter systems described by partial differential equations [18,19].

Systems with delay are infinite-dimensional and their stability analysis usually leads to transcendental equations with an infinite number of roots. The solution of these equations to locate their roots is of interest in determining the stability of a system; see for example [20–22] and the literature cited therein. In [23], a transcendental equation has been solved to construct a PI controller to stabilize first-order plants with input delay. In [24], the thermal aspects of long duct flows with constant mass flow have been addressed.

In this work temperature control at the outlet of a long duct by manipulation of the flow velocity is studied. The problem would have been linear if either the inlet or ambient temperature were the control input, but in the present case it is non-linear [25–27]. The residence time of the fluid in the duct is variable leading to a variable delay between the moment the fluid enters and when it leaves the duct. The controller changes the fluid velocity and through that the residence time. Linear stability analysis will be carried out with small perturbations while non-linear effects will be determined numerically.

2. Governing equations

Let us consider a duct of constant cross-section schematically shown in Fig. 1 where the flow is driven by a variable-speed pump. The fluid inlet temperature T_{in} is kept constant, and there is heat loss to the ambient at temperature T_∞ through the surface of the duct. To enable a simplified, one-dimensional analysis, the assumptions that the velocity and temperature are uniform over the cross-section of the pipe, and that the flow is hydrodynamically and thermally fully developed are made. The physical properties of the fluid and the coefficient of heat transfer to the ambient are also constant. Though it is not necessary to write or solve the governing equations in both Eulerian and Lagrangian frames since they are equivalent, it is instructive and useful to do so.

2.1. Eulerian

On neglecting axial conduction, energy conservation gives [24]

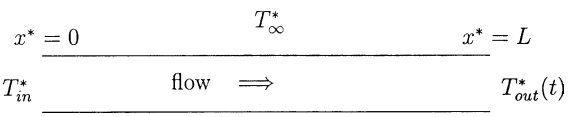

Fig. 1. Schematic of duct.

$$\frac{\partial T^*}{\partial t^*} + v^* \frac{\partial T^*}{\partial x^*} + \frac{4h}{\rho c D}(T^* - T^*_\infty) = 0, \tag{1}$$

where $T^*(x^*, t^*)$ is the fluid temperature, t^* is time, x^* is the distance along the duct measured from the entrance, $v^*(t^*)$ is the flow velocity, h is the coefficient of heat transfer to the exterior, ρ is the fluid density, c is its specific heat at constant pressure, and D is the hydraulic diameter of the duct. The duct is assumed to be of uniform cross-section so that for an incompressible fluid the flow velocity v^* is not a function of x^*. Also v^* is taken to be always positive, so that the $x^* = 0$ end is always the inlet; this fixes the boundary condition as $T^*(0, t^*) = T^*_{\text{in}}$. The temperature of the fluid coming out of the duct is $T^*(L, t^*) = T^*_{\text{out}}(t^*)$, where L is the length of the duct.

Using the non-dimensional variables $x = x^*/L$, $T = (T^* - T^*_\infty)/(T^*_{\text{in}} - T^*_\infty)$, $t = t^* 4h/\rho c D$, and $v = v^* \rho c D/hL$, Eq. (1) becomes

$$\frac{\partial T}{\partial t} + v \frac{\partial T}{\partial x} + T = 0, \tag{2}$$

with $T(0, t) = 1$. This is an equation in $T(x, t)$ if $v(t)$ is known. After the initial startup period in which the fluid within the duct is flushed out, the general solution is

$$T(x, t) = \mathrm{e}^{-t} f\left(x - \int_0^t v(s)\,\mathrm{d}s\right), \tag{3}$$

where f is an arbitrary function. Applying the boundary condition at $x = 0$ gives

$$1 = \mathrm{e}^{-t} f\left(-\int_0^t v(s)\,\mathrm{d}s\right). \tag{4}$$

In general, f is an implicit function of t and cannot be explicitly determined and thus cannot be eliminated between the two equations. The temperature at the outlet of the duct, i.e. at $x = 1$, is

$$T_{\text{out}}(t) = \mathrm{e}^{-t} f\left(1 - \int_0^t v(s)\,\mathrm{d}s\right). \tag{5}$$

Eqs. (4) and (5) must be simultaneously solved to get the outlet temperature $T_{\text{out}}(t)$ in terms of the flow velocity $v(t)$.

2.2. Lagrangian

In this formulation, Eq. (2) becomes

$$\frac{\mathrm{D}T}{\mathrm{D}t} + T = 0, \tag{6}$$

where $\mathrm{D}/\mathrm{D}t = \partial/\partial t + v\,\partial/\partial x$ is the derivative following the fluid. Since the inlet temperature is unity, this can be integrated as

$$T(t) = \mathrm{e}^{-t}, \tag{7}$$

to give the temperature of a fluid particle t units of time after it has entered the duct.

At the outlet this becomes

$$T_{\text{out}}(t) = \mathrm{e}^{-\tau(t)}, \tag{8}$$

where $\tau(t)$ is the residence time, i.e. the time taken for a fluid particle to go from inlet to outlet. Since the fluid exiting the duct at time t was within the duct during the interval from the instant $t - \tau$ to the present, we also have

$$\int_{t-\tau}^{t} v(s)\,\mathrm{d}s = 1. \tag{9}$$

If $v(t)$ is known, this defines the residence time $\tau(t)$ which can then be substituted into Eq. (8) to determine the outlet temperature.

2.3. Discussion

Both formulations have their advantages: the Eulerian shows the explicit effect of advection and the Lagrangian the residence time. To show that the two formulations are equivalent, Eqs. (5) and (8) can be combined to give

$$f\left(1 - \int_0^t v(s)\,\mathrm{d}s\right) = \mathrm{e}^{t-\tau}, \tag{10}$$

which in principle can be inverted as

$$1 - \int_0^t v(s)\,\mathrm{d}s = g(\mathrm{e}^{t-\tau}). \tag{11}$$

On the other hand, Eq. (4) gives

$$-\int_0^t v(s)\,\mathrm{d}s = g(\mathrm{e}^t). \tag{12}$$

Thus

$$\begin{aligned}\int_{t-\tau}^{t} v(s)\,\mathrm{d}s &= \int_0^t v(s)\,\mathrm{d}s - \int_0^{t-\tau} v(s)\,\mathrm{d}s \\ &= g(\mathrm{e}^{t-\tau}) - g(\mathrm{e}^t) = 1,\end{aligned} \tag{13}$$

which is Eq. (9).

In the previous solutions, $v(t)$ has been assumed to be known. However, in a control problem in which the flow velocity is the control input, it is related to some function of the error through an additional equation that governs the controller. It must be pointed out also that in that case, Eq. (2) is non-linear and Eq. (9) has a dependent variable $\tau(t)$ in one of the limits of the integral.

3. Numerical solutions

Simulations are used to solve the non-linear problem to determine the temperature $T(x, t)$, flow velocity $v(t)$ and residence time $\tau(t)$. When necessary, the duct is initially assumed to be at unit temperature so that the initial condition is $T(x, 0) = 1$.

3.1. Procedures

Discretizing in space and time, a finite-difference approximation can be used to solve the Eulerian formulation Eq. (2). An upwind scheme gives

$$T_i^{j+1} = (1 + \Delta t - \varepsilon)T_i^j + \varepsilon T_{i-1}^j. \tag{14}$$

The subscripts increase in the flow direction and denote discretization points in space, superscripts denote time, $\varepsilon = v\Delta t/\Delta x$, Δt is the time step, and $\Delta x = 1/N$ is the spatial grid size, where N is the number of uniform spatial divisions. The Courant–Friedrichs–Lévy condition [14] for stability of the numerical scheme is $\Delta t \leqslant \Delta x/\max\{v(t)\}$.

To solve the Lagrangian Eq. (6), the duct is discretized only in space. The time interval that takes the fluid particle at any grid point to the downstream neighboring grid point is

$$\Delta t^j = \frac{\Delta x}{v}. \tag{15}$$

On following a fluid particle, the solution of Eq. (6), over this interval of time gives

$$T_i^j = T_{i-1}^{j-1}\exp(-\Delta t^j). \tag{16}$$

Thus Δx is fixed, but Δt^j at each time step is determined from Eq. (15). If v is not given but related by an additional control equation, it is possible to use either an explicit procedure in which $v = v^{j-1}$ (i.e. at the previous time step), or implicit where $v = v^j$. The latter is used here with a suitable number of iterations until there is convergence in v^j.

3.2. Validation

To reduce the possibility of numerical errors in the results, especially in the sensitive sub-critical computations, the numerical solutions should validated. As a steady-state test, the analytical solution of the temperature distribution for constant velocity is checked against the numerical. For time-dependent v, solutions from the Eulerian and Lagrangian methods described above were compared for

$$v(t) = \begin{cases} 0.5 & \text{for } t \leqslant 1, \\ 2 & \text{for } t > 1. \end{cases} \tag{17}$$

Both formulations converged for increasing N, and a value of 100 will be used in the computations. However, since the Lagrangian method uses the exact solution to compute the particle temperature as it moves, it is more accurate in the representation of temperature distributions that are not differentiable in space and for this reason it is used for the computations that follow.

3.3. Open-loop dynamics

Figs. 2 and 3 show the temporal and spatial characteristics of $T(x,t)$ for $v(t)$ in Eq. (17). The steady-state

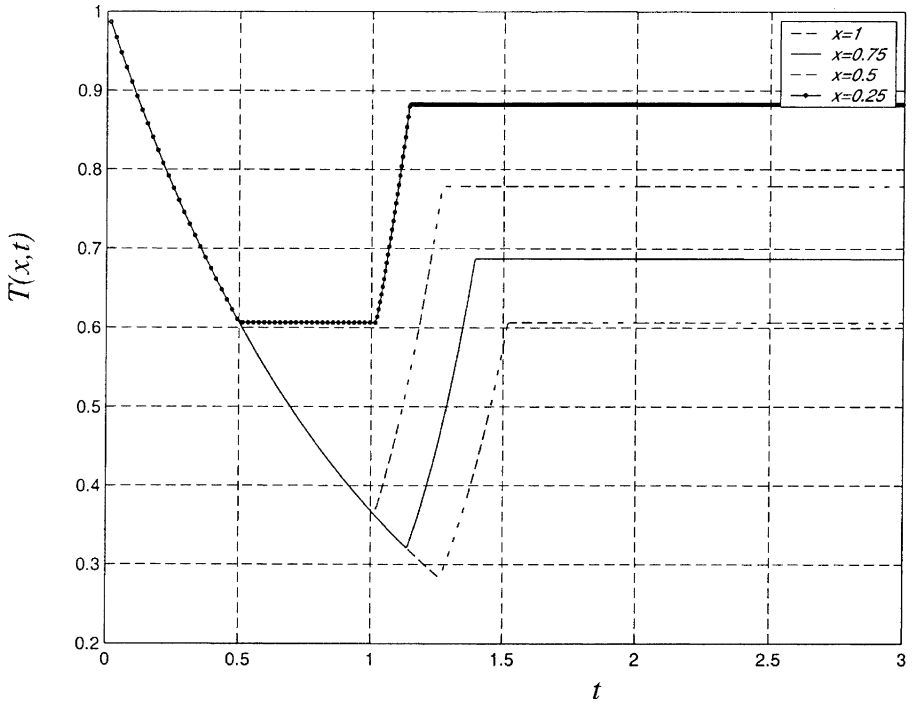

Fig. 2. Open-loop response: temporal dependence of temperature $T(x,t)$ at different locations for step change in $v(t)$ at $t = 1$.

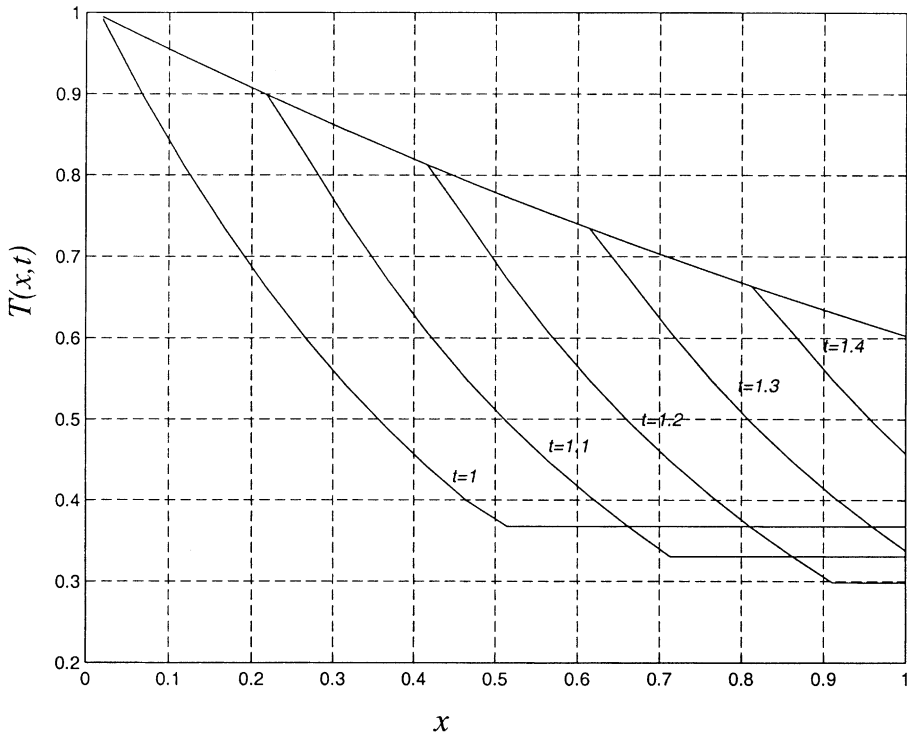

Fig. 3. Open-loop response: spatial dependence of temperature $T(x,t)$ at different times for step change in $v(t)$ at $t = 1$.

temperature distribution for a constant $v(t) = \bar{v}$ is $\overline{T}(x) = e^{-x/\bar{v}}$, so that $\overline{T}_{out} = e^{-1/\bar{v}}$. $T(x,t)$ and $T_{out}(t)$ approach $\overline{T}(x) = e^{-x/0.5}$ and $\overline{T}_{out} = e^{-1/0.5}$ up to $t = 1$; after that they tend to $\overline{T}(x) = e^{-x/2}$ and $\overline{T}_{out} = e^{-1/2}$. The temperature pattern is seen to advect downstream due to the fluid motion as well as decrease due to heat loss to the ambient. The control system has to deal with both these phenomena.

4. Outlet temperature control

The objective of control is assumed to be the regulation of the outlet temperature, T_{out}, to a constant value by altering the flow velocity $v(t)$. Since $0 < \tau < \infty$, Eq. (8) shows that $1 > T_{out}(t) > 0$. Thus only this range of values of the outlet temperature can be reached by varying the flow velocity, and that it is controllable at most within this range. This is in contrast to a controllable linear system where in theory its state can be changed from any value to any other.

Variables for the desired steady state of the system are indicated by overbars, i.e. $v = \bar{v}$, $\tau = \bar{\tau}$ and $T_{out} = \overline{T}_{out}$. From Eqs. (8) and (9) they are related by $\overline{T}_{out} = e^{-\bar{\tau}}$ and $\bar{v}\bar{\tau} = 1$. By changing $v(t)$ it is desired to maintain $\overline{T}_{out}$ as the outlet temperature in spite of any disturbances. Different strategies can be used for this purpose, but here the commonly-used Proportional-Integral (PI) control will be employed. In this case the flow velocity is related to the error $e(t) = T_{out}(t) - \overline{T}_{out}$ by

$$v(t) = K_p e(t) + K_i \int_0^t e(s)\,ds, \tag{18}$$

the differential form of which is

$$\frac{dv}{dt} = K_p \frac{de}{dt} + K_i e(t). \tag{19}$$

5. Linear stability analysis

The linear stability of this control system can be analyzed by applying small perturbations of the form $T_{out}(t) = \overline{T}_{out} + T'_{out}(t)$, $\tau(t) = \bar{\tau} + \tau'(t)$ and $v(t) = \bar{v} + v'(t)$. Substituting in Eqs. (8) and (9), neglecting the higher-order terms, and subtracting out the steady states, the perturbation equations

$$T'_{out}(t) + e^{-\bar{\tau}}\tau'(t) = 0, \tag{20}$$

$$\int_{t-\bar{\tau}}^{t} v'(s)\,ds + \bar{v}\tau'(t) = 0 \tag{21}$$

are obtained. From Eq. (19) and the above it can be shown that

$$\frac{dv'}{dt} = -e^{-\bar{\tau}}\left(K_p\frac{d\tau'}{dt} + K_i\tau'\right) = \frac{K_p e^{-\bar{\tau}}}{\bar{v}}(v'(t) - v'(t-\bar{\tau})) + \frac{K_i e^{-\bar{\tau}}}{\bar{v}}\int_{t-\bar{\tau}}^{t} v'(s)\,ds. \quad (22)$$

Writing $v'(t) = \hat{v}e^{\sigma t}$, a transcendental equation

$$F(\sigma) = \sigma - \bar{\tau}e^{-\bar{\tau}}\left(K_p + \frac{K_i}{\sigma}\right)(1 - e^{-\sigma\bar{\tau}}) = 0 \quad (23)$$

for the eigenvalues σ is obtained. In general, this has an infinite number of roots that cannot be explicitly written down. For stability the real part of the roots of σ should be negative. The values of the roots depend on the residence time $\bar{\tau}$ and the control parameters K_p and K_i.

5.1. Pontryagin's method

Recent work on the zeros of exponential polynomials based on that of Pontryagin [21,23,28] will be used to determine whether the real parts of the roots of σ are negative or not. To put the transcendental function in an appropriate form, $F^*(\sigma) = \sigma F(\sigma)e^{\sigma\bar{\tau}}$ is defined so that

$$F^*(\sigma) = (\sigma^2 - \bar{\tau}e^{-\bar{\tau}}K_p\sigma - \bar{\tau}e^{-\bar{\tau}}K_i)e^{\sigma\bar{\tau}} + \bar{\tau}e^{-\bar{\tau}}(K_p\sigma + K_i) = 0. \quad (24)$$

Eq. (24) has one extra root at the origin compared to Eq. (23). The following theorems, slightly modified from Silva et al. [23], give the necessary and sufficient conditions for the roots of Eq. (24) to have negative real parts.

Theorem A. *Let $F^*(\sigma)$ be written as $F_r^*(\omega) + iF_i^*(\omega)$, where $\sigma = i\omega$ and ω, F_r^* and F_i^* are real. Then, $F^* = 0$ has roots in the negative half of the complex plane if and only if the following two conditions are satisfied: (i) $F_r^* = 0$ and $F_i^* = 0$ have only simple real roots and these interlace, and (ii) $F_r^*(dF_i^*/d\omega) - F_i^*(dF_r^*/d\omega) > 0$, for some ω in $(-\infty, \infty)$.*

To ensure that $F_r^* = 0$ and $F_i^* = 0$ have only real roots, the following theorem can be used.

Theorem B. *Let M_1 and M_2 denote the highest power of σ and e^{σ}, respectively, in $F^*(\sigma)$, and ϵ be an appropriate constant such that the coefficient of terms of highest degree in F_r^* and F_i^* do not vanish at $\omega = \epsilon$. Then, for the equations $F_r^* = 0$ and $F_i^* = 0$ to have only real roots, it is necessary and sufficient that in the interval $-2k\pi + \epsilon \leqslant \omega \leqslant 2k\pi + \epsilon$, $F_r^* = 0$ and $F_i^* = 0$ have exactly $M_1 + 4kM_2$ real roots starting with a sufficiently large integer k.*

To apply the technique, it must first be shown using **B** that for specific values of the parameters, F_r^* and F_i^* satisfy condition **A**(i). The extra root $\sigma = 0$ in $F^* = 0$ must be subtracted from the total number required in any interval by the above theorem. Writing $\sigma = i\omega$ in Eq. (24), we have

$$F_r^*(\omega) = -\cos\omega\bar{\tau}(\omega^2 + \bar{\tau}e^{-\bar{\tau}}K_i) + \bar{\tau}e^{-\bar{\tau}}K_p\omega\sin\omega\bar{\tau} + \bar{\tau}e^{-\bar{\tau}}K_i, \quad (25)$$

$$F_i^*(\omega) = -\sin\omega\bar{\tau}(\omega^2 + \bar{\tau}e^{-\bar{\tau}}K_i) - \bar{\tau}e^{-\bar{\tau}}K_p\omega\cos\omega\bar{\tau} + \bar{\tau}e^{-\bar{\tau}}K_p\omega, \quad (26)$$

where the principal terms are $-\omega^2\cos\omega$ and $-\omega^2\sin\omega$ respectively. We choose $\epsilon = \pi/4$ such that the principal terms do not vanish there. For $k = 1$, graphs of F_r^* and F_i^* are plotted to find the number of zeros (excluding the one at zero) in the interval $-2k\pi + \epsilon \leqslant \omega \leqslant 2k\pi + \epsilon$. The number increases by 4, and continues to increase by 4 as k is increased by 1. In addition, the interlacing of the zeros of F_r^* and F_i^* is clear from these graphs. This completes condition **A**(i). The inequality **A**(ii) is also easily checked by computation. Examples of graphs of F_r^*, F_i^* and $F_r^*(dF_i^*/d\omega) - F_i^*(dF_r^*/d\omega)$ are shown in [25].

5.2. Neutral stability

Eq. (23) can be used for a quantitative estimate of the frequency of the oscillations that appear during Hopf bifurcations. Let σ and $F(\sigma)$ be separated into their real and imaginary parts to give

$$\sigma_r - \bar{\tau}e^{\bar{\tau}}K_p + \bar{\tau}e^{\bar{\tau}}K_p e^{-\sigma_r\bar{\tau}}\cos\sigma_i\bar{\tau} - \frac{\bar{\tau}e^{\bar{\tau}}K_i\sigma_r}{\sigma_r^2 + \sigma_i^2} + \frac{\bar{\tau}e^{\bar{\tau}}K_i}{\sigma_r^2 + \sigma_i^2}(\sigma_r\cos\sigma_i\bar{\tau} - \sigma_i\sin\sigma_i\bar{\tau}) = 0, \quad (27)$$

$$\sigma_i - \bar{\tau}e^{\bar{\tau}}K_p e^{-\sigma_r\bar{\tau}}\sin\sigma_i\bar{\tau} + \frac{\bar{\tau}e^{\bar{\tau}}K_i\sigma_i}{\sigma_r^2 + \sigma_i^2} - \frac{\bar{\tau}e^{\bar{\tau}}K_i}{\sigma_r^2 + \sigma_i^2} \times (\sigma_i\cos\sigma_i\bar{\tau} + \sigma_r\sin\sigma_i\bar{\tau}) = 0, \quad (28)$$

where $\sigma = \sigma_r + i\sigma_i$. For neutral stability $\sigma_r = 0$, so that the above equations become

$$-\bar{\tau}e^{\bar{\tau}}K_p(1 - \cos\sigma_i\bar{\tau}) - \frac{\bar{\tau}e^{\bar{\tau}}K_i}{\sigma_i}\sin\sigma_i\bar{\tau} = 0, \quad (29)$$

$$\sigma_i - \bar{\tau}e^{\bar{\tau}}K_p\sin\sigma_i\bar{\tau} + \frac{\bar{\tau}e^{\bar{\tau}}K_i}{\sigma_i}(1 - \cos\sigma_i\bar{\tau}) = 0. \quad (30)$$

Manipulation of these equations yields

$$\sigma_i = \pm\sqrt{-2\bar{\tau}e^{-\bar{\tau}}K_i}. \quad (31)$$

6. Linear stability results

Three different cases can be studied for different values of $\bar{\tau}$, and for each the stability results will be determined as a function of the system parameters.

6.1. $\overline{\tau} \ll 1$

For small residence times, the exponentials in Eq. (23) can be expanded to give

$$\sigma = -\frac{2}{K_p \overline{\tau}^3} + \frac{2}{\overline{\tau}} - \left(2 + \frac{K_i}{K_p}\right) - K_i \overline{\tau}^2 + K_i \overline{\tau}^3 + O(\overline{\tau}^4). \tag{32}$$

Thus σ is real, and the control system is stable only if $(K_i \overline{\tau}^3 + 2)/K_p < 2\overline{\tau}^2(1 - \overline{\tau})$. This is shown in Fig. 4 for two different $\overline{\tau}$s. It is observed that the range of stability increases as $\overline{\tau}$ decreases. When $\overline{\tau} \to 0$, the stability region will cover the entire (K_i, K_p) parameter space, and the system is unconditionally stable. This also clear from Eq. (23), though one should be careful since $\overline{\tau} = 0$ in the equation is not exactly the same as $\overline{\tau} \to 0$. A vanishingly small $\overline{\tau}$ means that the flow is fast enough so that the time spent by a fluid particle within the duct is negligible.

6.2. $\overline{\tau} = O(1)$

The transcendental Eq. (23) may now have real or complex roots. The location of the roots and thus the stability of the system is examined using Pontryagin's method; details are in [25]. The resulting stability map in the (K_i, K_p) plane is shown in Fig. 5. The positive and negative K_i regions are studied separately.

(a) $K_i > 0$: Eq. (31) shows that real values of σ_i are not possible in this parameter region meaning that there is no portion of the neutral stability curve here. Graphs of $F(\sigma)$ as well as Pontryagin's theorem show that $F(\sigma) = 0$ has real, positive roots, so that the system is unstable for this entire region.

(b) $K_i < 0$: From Eq. (31) it can be seen that neutral stability is possible in this region. $F(\sigma) = 0$ may have complex roots; Pontryagin's method and repeated plotting are used to find the parameter ranges for which they lie on the negative left half of the complex plane.

6.3. $\overline{\tau} \gg 1$

For very large $\overline{\tau}$ the exponentials in Eq. (23) tend to zero, so that $\sigma \to 0$. The system is stable. However, $\overline{T}_{out} \to 0$ at the same time, meaning that the outlet temperature tends to the ambient. The system under these conditions, though stable, is not very useful for heating or cooling purposes.

6.4. Discussion

The stability of the control system for $\overline{\tau} \ll 1$, O(1) and $\gg 1$ has been investigated, and it is found that it is stable for both large and small $\overline{\tau}$, but can be unstable in the

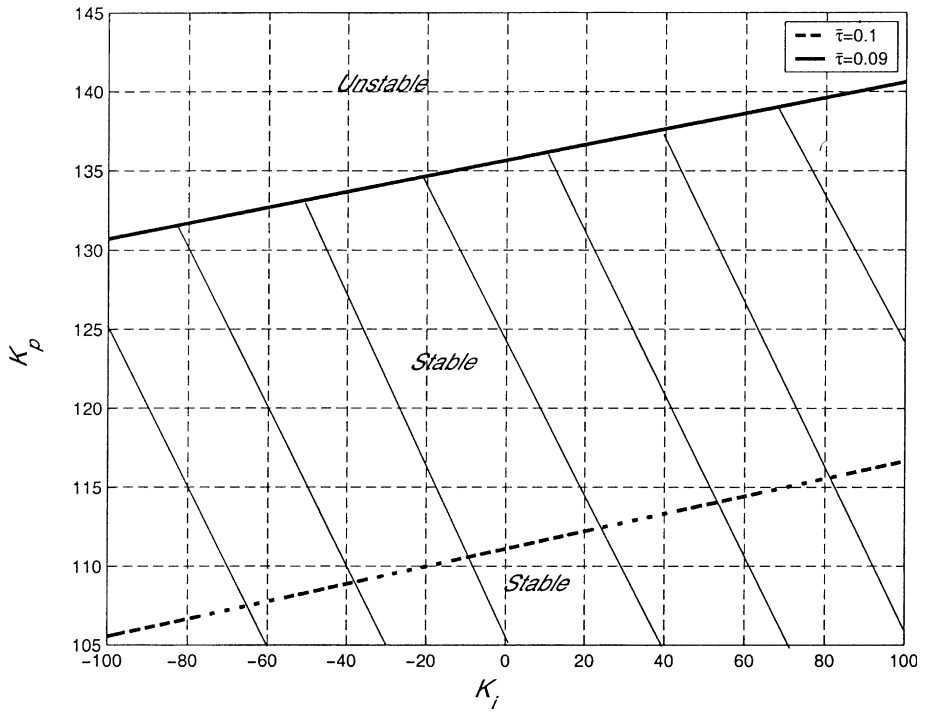

Fig. 4. Stability boundary for $\overline{\tau} \ll 1$.

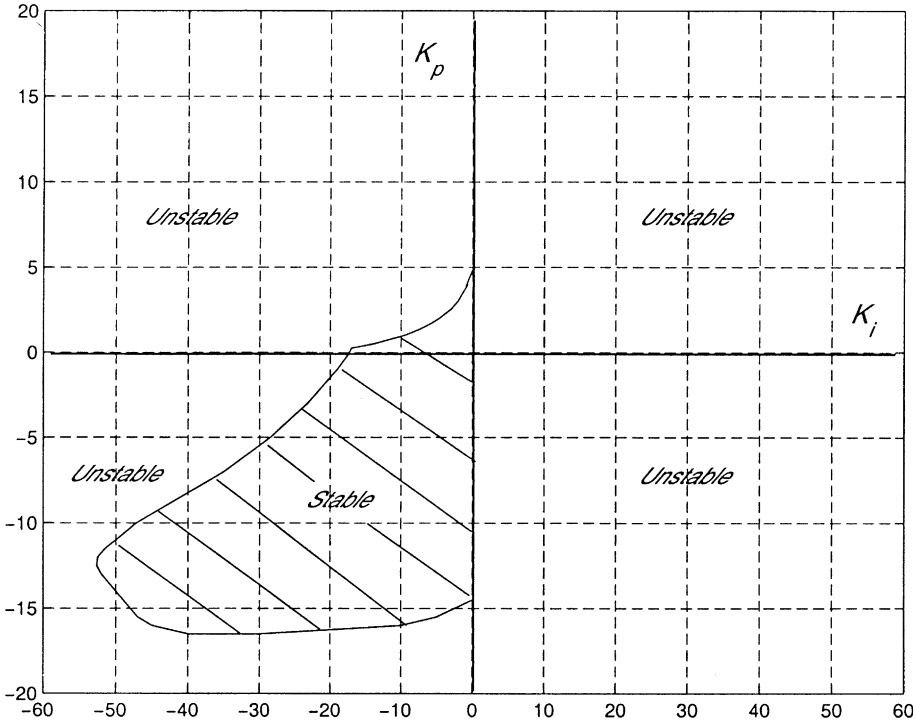

Fig. 5. Stability map for $\bar{\tau} = 1$.

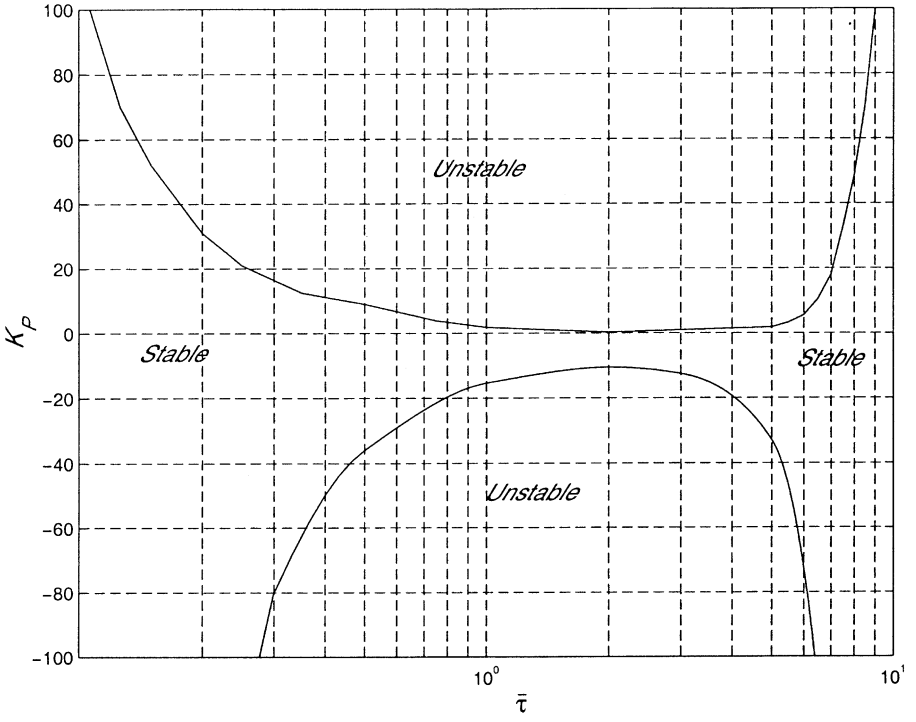

Fig. 6. Effect of $\bar{\tau}$ for constant $K_i = -5$ and variable K_p.

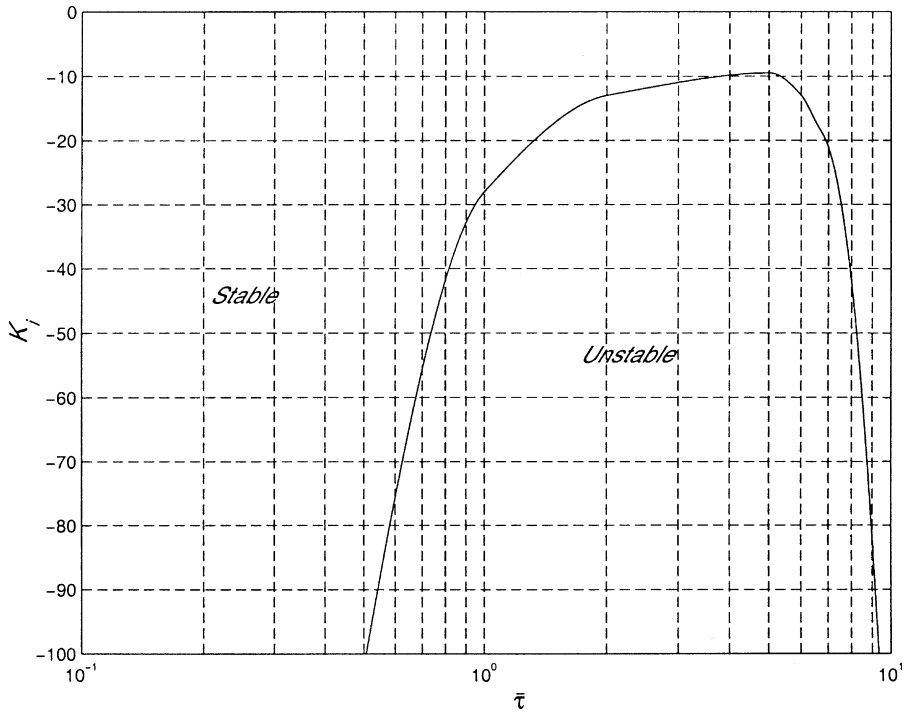

Fig. 7. Effect of $\bar{\tau}$ for variable K_i and constant $K_p = -5$.

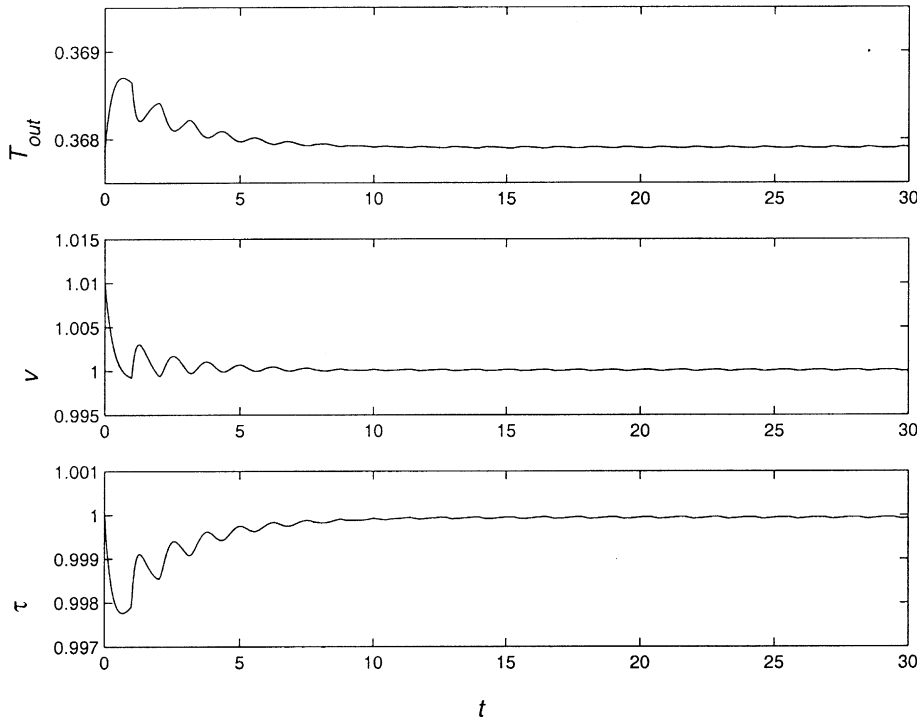

Fig. 8. Outlet temperature $T_{out}(t)$, flow velocity $v(t)$, and residence time $\tau(t)$ for $\bar{\tau} = 1$, $K_i = -5$ and $K_p = 1.5$.

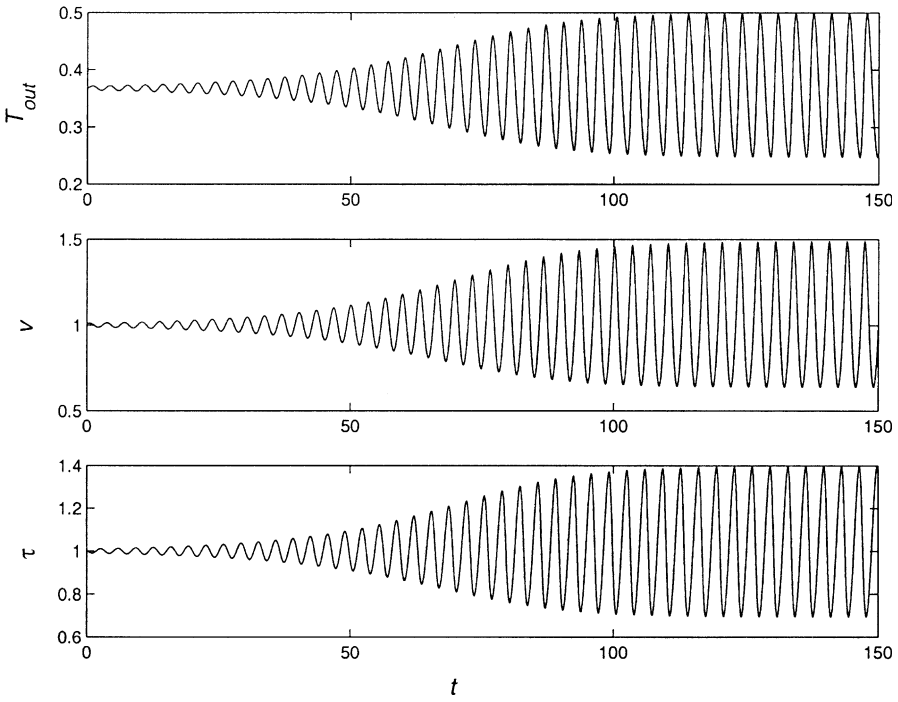

Fig. 9. Outlet temperature $T_{\text{out}}(t)$, velocity $v(t)$, and residence time $\tau(t)$ for $\overline{\tau} = 1$, $K_{\text{i}} = -5$ and $K_{\text{p}} = 2.5$.

middle. The O(1) stability map shown in Fig. 5 needs further discussion. Eq. (31) shows that loss of stability occurs through two different types of bifurcations. When $K_{\text{i}} < 0$ there are two complex roots for σ that cross the imaginary axis. This is a Hopf bifurcation that indicates an oscillatory behavior of the system. On the other hand if $K_{\text{i}} = 0$, then $\sigma_{\text{i}} = 0$ and a simple bifurcation occurs.

The effect of $\overline{\tau}$ on system stability is shown in Figs. 6 and 7 as a function of K_{p} and K_{i} respectively. In Fig. 6 large stability regions can be seen for both small and large $\overline{\tau}$. A similar behavior is also shown in Fig. 7, but with stability possible only for $K_{\text{i}} < 0$.

7. Numerical results

To verify and extend analytical results, the dynamical behavior of the control system in response to perturbations will be examined numerically. The target temperature at the outlet of the duct was set at $\overline{T}_{\text{out}} = \text{e}^{-1}$, and after having the system stabilized at a steady-state temperature distribution and velocity, a small change in the inlet velocity of the order of one percent is introduced. The temperature distribution $T(x,t)$, the flow velocity $v(t)$ and the residence time $\tau(t)$ are determined as a function of time. If the system is asymptotically stable, the controller brings the system back towards the steady-state condition, and the effect of the perturbation vanishes exponentially with time. The numerical method cannot only examine linear stability to vanishingly small perturbations which was studied in the previous two sections (for which the analytical and computed results coincide), but also non-linear behavior for which the magnitude of the perturbation determines system stability. Thus super- and sub-critical bifurcations can be distinguished, something that cannot be done by linear analysis. In addition, numerical results enable the large-time dynamics of the system under unstable conditions to be determined.

7.1. Super-critical bifurcations

Here the stability of the solutions near the boundary does not depend on the amplitude of the perturbation. Most of the stability boundaries in Fig. 5 are of this type, and Figs. 8–14 show the response of the system near these parts for $\overline{\tau} = 1$. The figures are in pairs, the first being the behavior in the stable and the second in the unstable side. The variables shown are $T_{\text{out}}(t)$, $v(t)$ and $\tau(t)$. Not shown is the function $T(x,t)$ which is part of the numerical solution and also varies dynamically in a corresponding manner.

(a) *$K_i < 0$ and $K_p > 0$ boundary:* Figs. 8 and 9 show the dynamic behavior of the system just below and above the neutral stability line, respectively. This

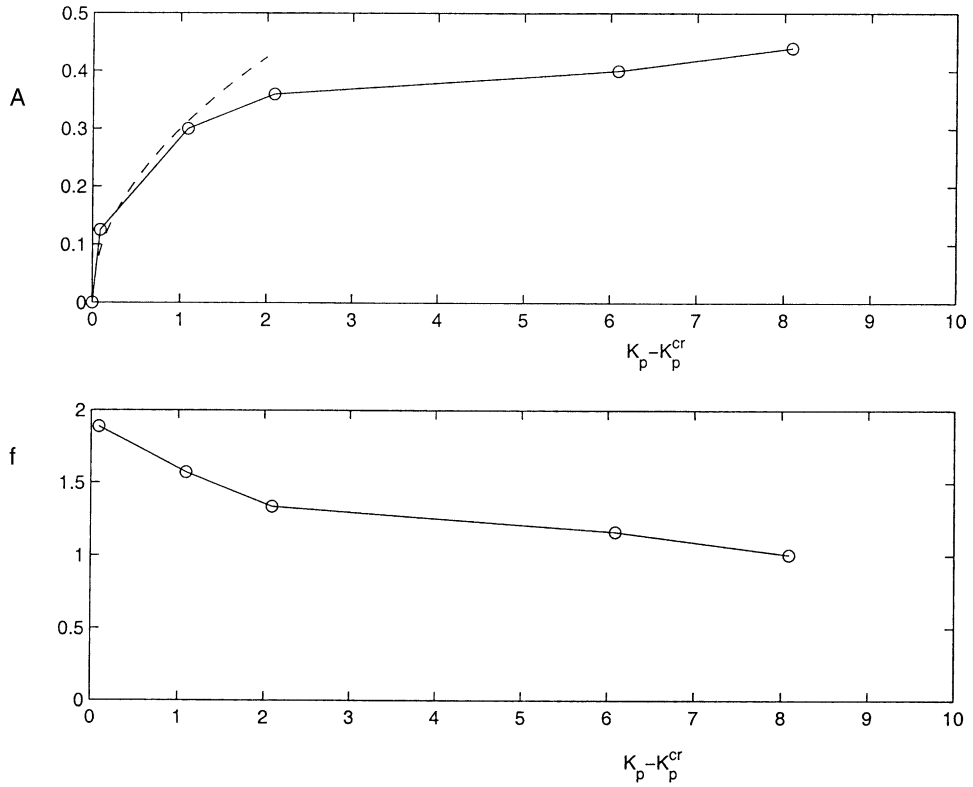

Fig. 10. Amplitude A and frequency f for $\bar{\tau} = 1$, $K_i = -5$ and $K_p^{cr} = 1.912$. A 1/2 power curve is shown by a dashed line in the amplitude plot.

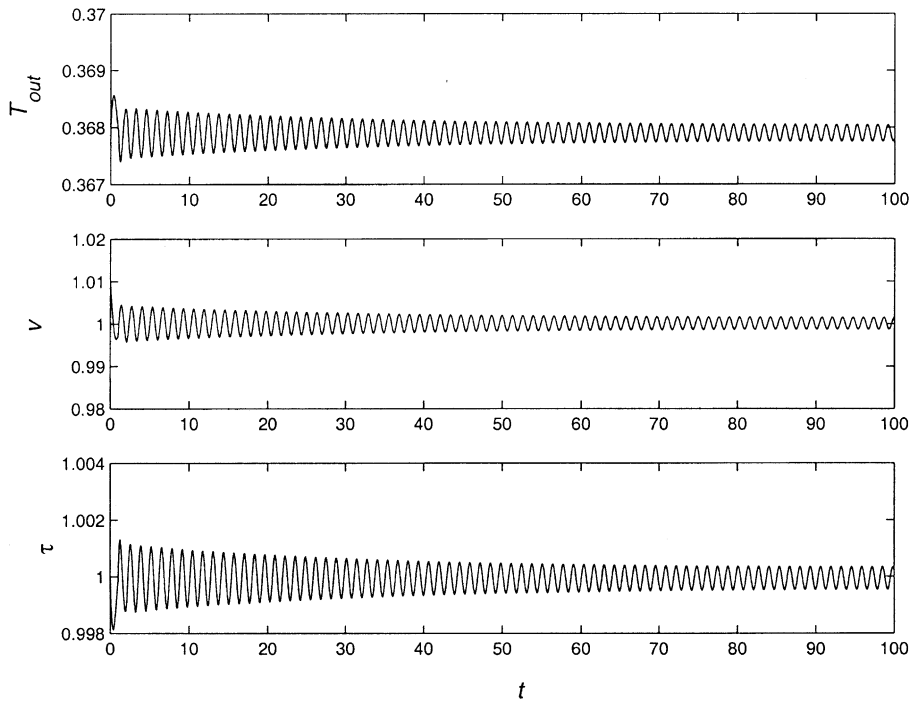

Fig. 11. Outlet temperature $T_{out}(t)$, velocity $v(t)$, and residence time $\tau(t)$ for $\bar{\tau} = 1$, $K_i = -30$ and $K_p = -7$.

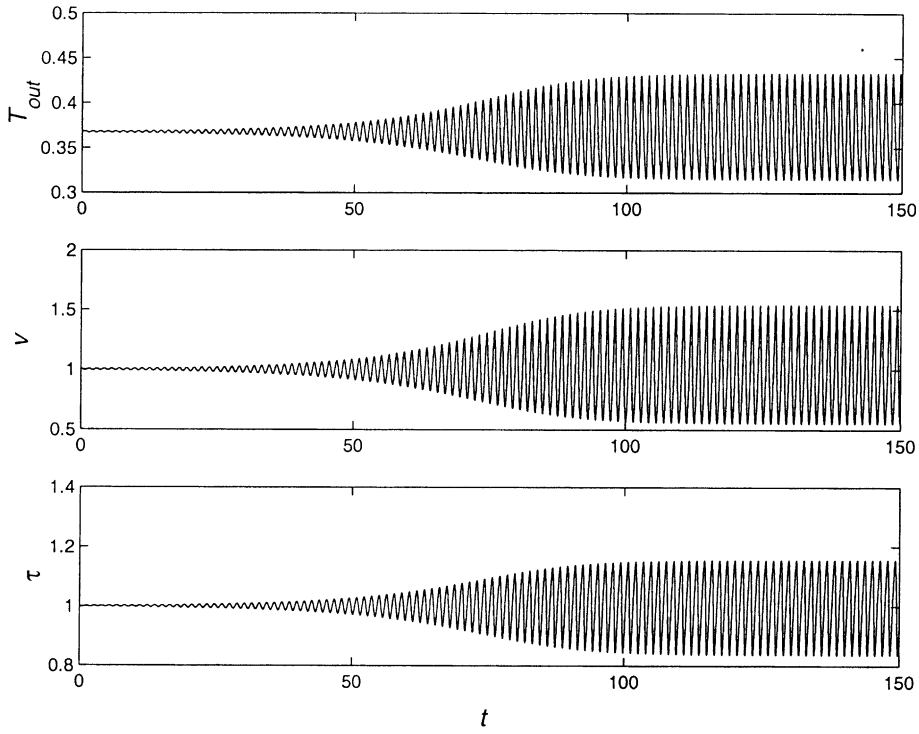

Fig. 12. Outlet temperature $T_{\text{out}}(t)$, velocity $v(t)$, and residence time $\tau(t)$ for $\overline{\tau} = 1$, $K_{\text{i}} = -30$ and $K_{\text{p}} = -5$.

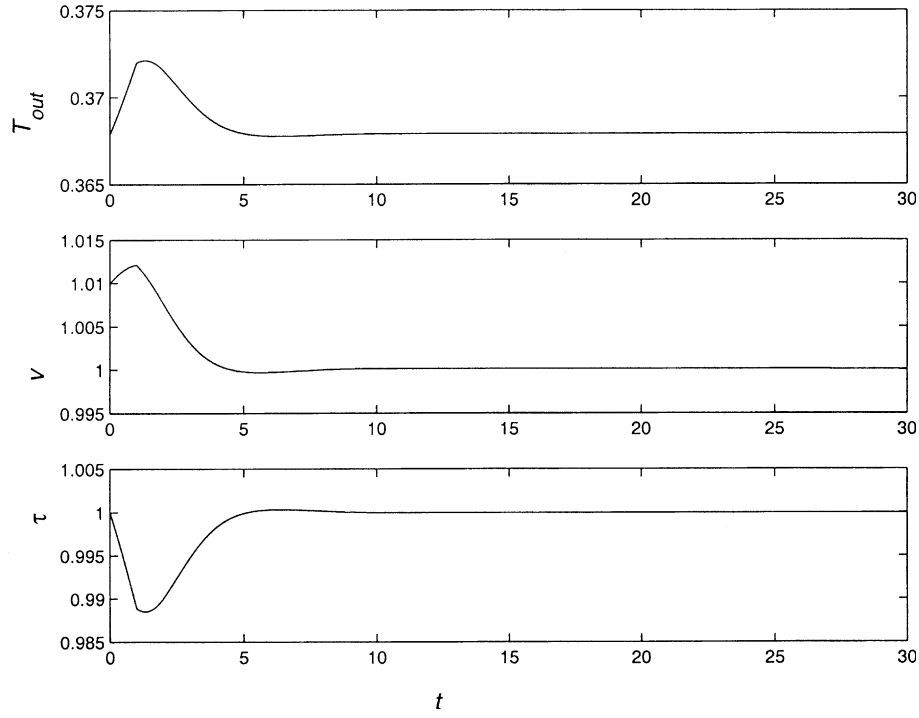

Fig. 13. Outlet temperature $T_{\text{out}}(t)$, velocity $v(t)$, and residence time $\tau(t)$ for $\overline{\tau} = 1$, $K_{\text{i}} = -1$ and $K_{\text{p}} = 1$.

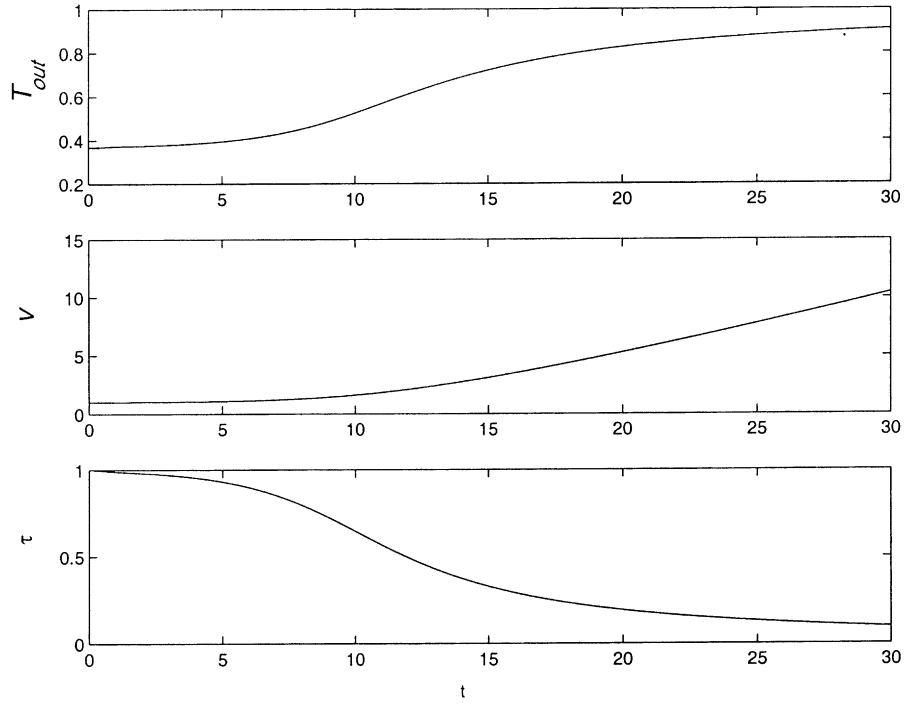

Fig. 14. Outlet temperature $T_{\text{out}}(t)$, velocity $v(t)$, and residence time $\tau(t)$ for $\overline{\tau} = 1$, $K_{\text{i}} = 1$ and $K_{\text{p}} = 1$.

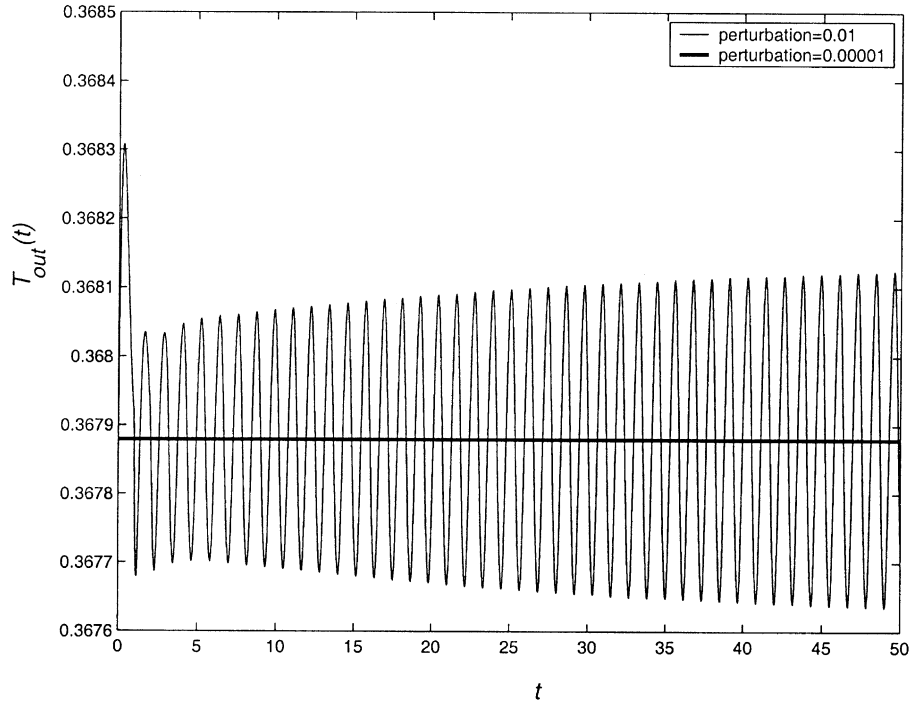

Fig. 15. Outlet temperature $T_{\text{out}}(t)$ at sub-critical Hopf bifurcation for $\overline{\tau} = 1$, $K_{\text{i}} = -40$ and $K_{\text{p}} = -15$.

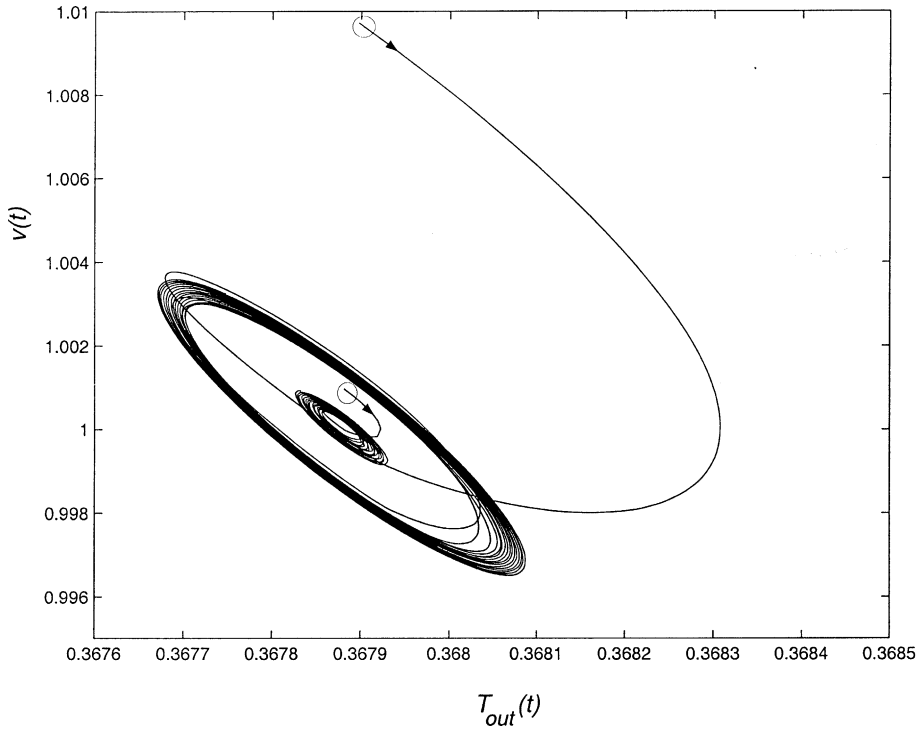

Fig. 16. Two sub-critical limit cycles for $\bar{\tau} = 1$, $K_i = -40$ and $K_p = -15$.

is a Hopf bifurcation and both figures show oscillations due to complex eigenvalues; however, in the stable side the oscillations damp out, while on the unstable side they grow to a finite amplitude limit cycle. The frequency roughly corresponds to that calculated from Eq. (31). As K_p and K_i move into the unstable region, the limit cycles get larger in amplitude. The amplitude and frequency of the finite-amplitude oscillations can be numerically determined. As an example, $K_i = -5$ was chosen for which the value of the parameter K_p at the stability boundary is $K_p^{cr} = 1.912$. For $K_p - K_p^{cr} > 0$ the time period of the oscillations increases and the frequency decreases. The amplitude A and frequency f are plotted as a function of $K_p - K_p^{cr}$ in Fig. 10.

(b) *$K_i < 0$ and $K_p < 0$ upper boundary:* This part of the stability boundary is also a super-critical Hopf bifurcation. Figs. 11 and 12 illustrate the behavior just inside and outside the boundary; the former shows damped oscillations and the latter oscillations that grow to a constant amplitude.

(c) *$K_i = 0$ boundary:* The eigenvalues are real, and hence there are no oscillations in the dynamic behavior of the system near this stability boundary. Figs. 13 and 14 show an example of the loss of stability at this boundary for $K_p > 0$. Similar behavior is also obtained for $K_p < 0$.

7.2. Sub-critical bifurcation

The lower stability boundary in the $K_i < 0$, $K_p < 0$ quadrant of Fig. 5 is different from the others in that it is sub-critical Hopf. The stability depends on the amplitude of the perturbation, and there is unstable behavior on the linearly stable side of the boundary if a large enough initial perturbation is provided. The dynamic behavior of $T_{out}(t)$ in this region is shown in Fig. 15. Two different perturbations of the steady state are shown: for a 10^{-3}% perturbation, no growth is observed in the response, while for 1% a steady, constant-amplitude limit-cycle oscillation is reached. A similar behavior is shown in Fig. 16 which plots the sub-critical limit cycles in a (T_{out}, v) phase-plane projection for two different initial conditions. Multiple long-time attractors with disjoint basins of attractions are observed to exist.

8. Conclusions

The PI control and stability of the outlet temperature of a long duct are investigated here with emphasis on the effect of the fluid residence time. The control input is the flow velocity which makes the problem non-linear. There is stability at the two extremes of small and large residence times and limited, conditional stability in the

middle. Usually delay destabilizes a system; in the beginning it does so in this case also, but as the residence time becomes very large the system becomes stable again. This gain in stability is at the expense of the reachability of the outlet temperature, the range of which ultimately shrinks to zero. It is also found that the system is not stable for any positive integral gain K_i.

Loss of stability at certain boundaries is through complex eigenvalues; both super- and sub-critical Hopf bifurcations are numerically found. The amplitude and frequency of the limit cycles are important to know in heating and cooling applications in which oscillations may be tolerated; it may be thus possible to work with parameter values for which the thermal system is actually unstable.

Though the Eulerian formulation Eq. (2) does not explicitly have a delay term, the Lagrangian version, as shown by Eq. (9), does. Caution must always be exercised in the study of the control behavior of plants modeled by partial differential equations with advective terms. Control inputs in one place at one instant in time affect the output behavior at another location at a later instant. This should be kept in mind when dealing with the thermal and flow control of more complex flows such as boundary layers, cavities or other multi-dimensional flows.

Acknowledgment

S.A. wishes to acknowledge financial support from Kuwait University.

References

[1] W. Munk, The delayed hot-water problem, ASME J. Appl. Mech. 21 (1954) 193, Brief notes.
[2] R. Górecki, J. Jekielek, Simplifying controller for process control of systems with large dead time, ISA Trans. 38 (1) (1999) 37–42.
[3] G.Y. Huang, L. Nie, Y.W. Zhao, Q.B. Wu, W.M. Yang, J. Liu, Temperature control system of heat exchangers, an application of DPS theory, Lecture Notes Control Inform. Sci. 159 (1991) 68–76.
[4] Z. Zhang, R.M. Nelson, Parametric analysis of a building space conditioned by a VAV system, ASHRAE Trans. 98 (1) (1992) 43–48.
[5] K.A. Antonopoulos, C. Tzivanidis, A correlation for the thermal delay of building, Renew. Energy 6 (7) (1995) 687–699.
[6] N. Saman, H. Mahdi, Analysis of the delay hot cold water problem, Energy 21 (5) (1996) 395–400.
[7] T.-T. Chow, F. Ip, A. Dunn, W.L. Tse, Numerical modeling of thermal behavior of fluid conduit flow with transport delay, ASHRAE Trans. 102 (2) (1996) 45–51.
[8] C. Comstock, On the delayed hot water problem, Wärme-Stoffübertr. 96 (1974) 166–171.
[9] J.A. Chu, Application of a discrete optimal tracking controller to an industrial electrical heater with pure delays, J. Process Control 5 (1) (1995) 3–8.
[10] J. Chu, H. Su, X. Hu, A time-delay control algorithm for an industrial electrical heater, J. Process Control 3 (4) (1993) 219–224.
[11] B.A. Ogunnaike, W.H. Ray, Process Dynamics, Modeling, and Control, Oxford University Press, New York, 1994.
[12] H.K. Rhee, N.R. Amundson, First-order Partial Differential Equations, Prentice-Hall, Englewood Cliffs, NJ, 1986.
[13] D. Russel, Quadratic performance criteria in boundary control of linear symmetric hyperbolic systems, SIAM J. Control 11 (3) (1973) 475–509.
[14] K.W. Morton, D.F. Mayers, Numerical Solution of Partial Differential Equations, Cambridge University Press, Cambridge, UK, 1994.
[15] A. Ito, H. Kanoh, M. Masubuchi, MWR approximation and modal control of parallel and counterflow heat exchangers, in: Proc. 2nd IFAC Symposium on Distributed-Parameter Systems, Pergamon, Oxford, 1978.
[16] M. Wysocki, Application of orthogonal collocation to simulation and control of first order hyperbolic systems, Math. Comput. Simul. 25 (4) (1983) 335–345.
[17] W.H. Ray, Advanced Process Control, McGraw-Hill, New York, 1981.
[18] P.D. Christofides, P. Daoutidis, Feedback control of hyperbolic PDE systems, AIChE J. 42 (11) (1996) 3063–3086.
[19] L. Irena, R. Triggiani, Deterministic Control Theory for Infinite Dimensional Systems, in: Encyclopedia of Mathematics, vol. I and II, Cambridge University Press, Cambridge, UK, 1999.
[20] B. Cahlon, D. Schmidt, On stability of systems of delay differential equations, J. Comput. Appl. Math. 117 (2) (2000) 137–158.
[21] M. Baptistini, P. Taboas, On the stability of some exponential polynomials, J. Math. Anal. Appl. 205 (1) (1997) 259–272.
[22] N. Silviu-Iulian, Delay Effects on Stability: A Robust Control Approach, in: Lecture Notes in Control and Information Sciences, Springer, London, 2001.
[23] G.J. Silva, A. Datta, S.P. Bhattacharyya, PI stabilization of first-order systems with time delay, Automatica 37 (12) (2001) 2025–2031.
[24] G. Díaz, M. Sen, K.T. Yang, R.L. McClain, Effect of delay in thermal systems with long ducts, Int. J. Thermal Sci. 43 (3) (2004) 249–254.
[25] S. Alotaibi, Temperature Controllability in Cross-Flow Heat Exchangers and Long Ducts, PhD Thesis, Department of Aerospace and Mechanical Engineering, University of Notre Dame, Notre Dame, IN, 2003.
[26] S. Alotaibi, M. Sen, B. Goodwine, K.T. Yang, Numerical simulation of the thermal control of heat exchangers, Numer. Heat Transfer A 41 (3) (2002) 229–244.
[27] S. Alotaibi, M. Sen, B. Goodwine, K.T. Yang, Controllability of cross-flow heat exchangers, Int. J. Heat Mass Transfer 47 (5) (2004) 913–924.
[28] R.E. Bellman, K.L. Cooke, Differential-Difference Equations, Academic Press, New York, 1963.